Biochimica et Biophysica Acta, 936 (1988) 249–258
Elsevier

BBA 42887

Electron spin polarization in the donor triplet state of bacterial photosynthetic reaction centres. II. Anisotropic inversion of electron spin polarization in a three-spin model reaction centre

P.J. Hore [a], David A. Hunter [a], Fred G.H. van Wijk [b,*], Tjeerd J. Schaafsma [b] and Arnold J. Hoff [c]

[a] *Physical Chemistry Laboratory, Oxford University, Oxford (U.K.),* [b] *Department of Molecular Physics, Wageningen Agricultural University, Wageningen and* [c] *Department of Biophysics, Huygens Laboratory, State University, Leiden (The Netherlands)*

(Received 5 August 1988)

Key words: Reaction center; Triplet state; Electron spin polarization; Iron-semiquinone complex; Spin-lattice relaxation; (*Rps. viridis*)

An explanation is proposed for the electron spin polarization pattern in the $\Delta m_S = \pm 1$ EPR spectrum of the donor triplet state in pre-reduced *Rhodopseudomonas viridis* reaction centres at temperatures above 20 K. Calculations based on a simple model of the reaction centre indicate that rapid spin-lattice relaxation of the iron-semiquinone complex ($Q_A^- Fe^{2+}$) can perturb the polarization of the donor triplet provided the EPR frequency of $Q_A^- Fe^{2+}$ is close to that of P^+ (the cation of the primary donor) and I^- (the anion of the intermediary acceptor). In agreement with experimental observations, this mechanism only operates in the presence of a large exchange interaction between I^- and $Q_A^- Fe^{2+}$. The observed anisotropy of this effect is attributed to the anisotropy of the resonance frequency of $Q_A^- Fe^{2+}$.

Introduction

The primary steps of bacterial photosynthesis may be summarised as follows:

$$\mathrm{PIX} \xrightarrow{h\nu} {}^1\mathrm{PIX} \rightarrow \mathrm{P}^+\mathrm{I}^-\mathrm{X} \rightarrow \mathrm{P}^+\mathrm{IX}^- \tag{1}$$

P, the primary electron donor, is a bacteriochlorophyll dimer with an electronically excited single state, ^{1}P. I is a bacteriopheophytin monomer and X is an iron-quinone complex, $Q_A Fe^{2+}$. When forward electron transfer from I^- to X is blocked, by reduction of X (to $X^- \equiv Q_A^- Fe^{2+}$), an excited triplet state of P (^{3}P) is formed by electron-hole recombination in the radical pair P^+I^-:

$$\mathrm{PIX}^- \xrightarrow{h\nu} {}^1\mathrm{PIX}^- \rightarrow \mathrm{P}^+\mathrm{I}^-\mathrm{X}^- \rightarrow {}^3\mathrm{PIX}^- \tag{2}$$

The donor triplet state is formed with strong electron spin polarization, as revealed by its electron paramagnetic resonance (EPR) spectrum [1,2] (for reviews, see Refs. 3–5). The steady-state polarization pattern of triplets created by continuous illumination at low temperatures (found in numerous photosynthetic systems, plants as well as bacteria) is denoted $\underset{\sim}{A}\underset{\sim}{E}\underset{\sim}{E}\underset{\sim}{A}\underset{\sim}{A}\underset{\sim}{E}$. $\underset{\sim}{A}$ signifies enhanced absorption and $\underset{\sim}{E}$ emission for the six resolvable features in the powder spectrum. This pattern has been satisfactorily explained in terms

---

[*] Present address: AKZO Research, Corporate Research Dept. (CRL), P.O. Box 60, 6800 AB Arnhem, The Netherlands.

Correspondence: T.J. Schaafsma, Department of Molecular Physics, Wageningen Agricultural University, De Dreijen 11, 6703 BC Wageningen, The Netherlands.

of the radical pair mechanism (RPM) [2] and indeed is sufficiently well understood that it is generally accepted as evidence for full photochemical activity in photosynthetic systems.

Recently, van Wijk et al. [6–9] found that the steady-state polarization of ^3P in pre-reduced *Rhodopseudomonas viridis* changed (to AEAEAE) at temperatures above about 20 K. From a variety of experiments it emerged that this inversion of the central portion of the spectrum only occurs when the $Q_A^-Fe^{2+}$ complex is intact and in the presence of a large exchange interaction between I^- and Q_A^-. More direct information on the origin of this effect is available from time-resolved EPR of the donor triplets formed by pulsed illumination, as described in the preceding paper (part I: Ref. 28). Using a 10 ns laser flash for excitation, initial electron spin polarizations could be detected at times (approx. 1 μs) short compared to the decay and spin-lattice relaxation times of the three triplet spin states, but long compared to the lifetime of the radical pair P^+I^- (approx. 10 ns in pre-reduced reaction centres [10,11]). Thus, while steady-state polarizations are complicated functions of the populating and de-populating rates of the triplet spin levels, the initial polarizations depend only on the relative populating rates of these states. At 8 K the initial polarization pattern is AEEAAE in agreement with the steady-state observation, while at 100 K it is –EAEA– where '–' indicates an absence of detectable signal. That is, the central portion of the spectrum is inverted while the two outer features have very little initial polarization.

It has been suggested [6–9] that rapid spin relaxation of paramagnetic Fe^{2+} is transmitted to P^+I^- via the $I^-Q_A^-$ coupling and that this disturbs the development of electron spin polarization in a way that is not completely understood. In what follows we provide theoretical support for this idea. We describe calculations that reproduce these curious effects in a model reaction centre, and offer some speculations on the mechanism of inversion.

Theory

We first review the origin of the 'conventional' AEEAAE polarization pattern, neglecting at this stage any effect of X^-. In high magnetic fields the appearance of the EPR spectrum of ^3P at thermal equilibrium is governed principally by the anisotropic zero-field splitting, i.e., the dipolar interaction between the two unpaired electron spins that comprise the triplet state. In this simple discussion *g*-tensor anisotropy and hyperfine interactions are ignored. The zero-field interaction causes the resonance frequency of ^3P to depend on its orientation in the magnetic field: the spectrum for a randomly oriented collection of triplets is shown schematically in Fig. 1A [12]. The main features are associated with the transitions occurring when the magnetic field is parallel to one of the principal axes of the zero-field splitting tensor. For each of the three principal directions (X, Y and Z) there are two components (+ and −) corresponding to the allowed transitions $|+1\rangle \rightarrow |0\rangle$ and $|0\rangle \leftarrow |-1\rangle$, respectively (the triplet spin states are labelled by the magnetic quantum number, m_S). To emphasize the six principal features and because the spectra to be discussed were all recorded using field modulation, we show the first derivative of this spectrum in Fig. 1B. As all transitions are in absorption at thermal equilibrium, this spectrum may be labelled AAAAAA.

To understand the AEEAAE polarized spectrum of ^3P one must consider the radical pair P^+P^-. This entity is formed from ^1P in a spin-correlated singlet state, $^1[P^+I^-]$, which must be converted into a triplet state, $^3[P^+I^-]$, before it can collapse to give ^3P (Fig. 2). Singlet–triplet interconversion in P^+I^- is brought about by hyperfine interactions which, at high field, produce $^3[P^+I^-]$ in its T_0 state ($m_S = 0$) only. Electron-hole recombination may then take place, with conservation of spin angular momentum, to give ^3P in state $|0\rangle$. In this simple picture, the other two states, $|+1\rangle$ and $|-1\rangle$ are not populated. Thus, the $|-1\rangle \leftarrow |0\rangle$ transitions are in enhanced absorption and the $|0\rangle \rightarrow |-1\rangle$ transitions are in emission: hence the AEEAAE pattern (Fig. 1C). The interconversion of singlet and triplet radical pair states in this way (known as the radical pair mechanism) is at the heart of the majority of electron-spin polarization effects in free radicals in liquids [13,14] as well as in photosynthetic systems [5] and also accounts for the effects of magnetic fields on chemical reaction yields [15,16].

The observation of AEAEAE (Fig. 1D) clearly requires that the central pair of peaks (Y^+ and Y^-) should have inverted polarization. That is, for triplets oriented such that the magnetic-field direction coincides with the Y axis of the zero-field splitting, the $|+1>$ and $|-1>$ states of ^3P must be more heavily populated than the $|0>$ state. Similarly, the –EAEA– initial polarization pattern indicates that when the magnetic field is along the Z axis of the zero-field splitting, the three states of ^3P must be almost equally populated. A large initial population of one of the triplet spin states can be identified with a rapid rate of formation of the corresponding state of $^3[P^+I^-]$.

The main theme of this paper will be to discover processes that can affect the rate of singlet–triplet interconversion in P^+I^- and in particular those that can cause the T_{+1} and T_{-1} ($m_S = \pm 1$) radical pair states to be formed more rapidly than T_0. To do this we have used a rather crude model of the bacterial reaction centre. Our philosophy has been to retain the basic minimum of interactions and properties necessary for anisotropic inversion of polarization and to ignore any interaction that did not seem to be essential; and our aim to discover the physical principles underlying this effect without trying to reproduce it quantitatively.

The calculation centres on the spin evolution and chemical dynamics of three unpaired electrons (each spin $\frac{1}{2}$), one on each of P^+, I^- and X^-. Fe^{2+} (spin 2) is not treated explicitly, even though it couples strongly to Q_A^- [17]. As basis states, we use the following combination of singlet and triplet states of P^+I^- and α and β ($m_S = \pm \frac{1}{2}$) states of X^-: $T_{+1}\alpha$, $T_{+1}\beta$, $T_0\alpha$, $T_0\beta$, $T_{-1}\alpha$, $T_{-1}\beta$, $S\alpha$, $S\beta$.

There are several sources of anisotropy in this three-spin system: probably the largest originate in X^- (zero-field splitting, Zeeman and exchange interactions). These interactions are modelled by allowing the g-value of X^- to be anisotropic. Calculations are in fact performed for different values of an isotropic g-value, $g(X^-)$, with the understanding that different g-values correspond to different (but unknown) orientations of the reaction centre in the magnetic field. All other anisotropic effects (e.g., dipolar interactions between P^+ and I^-, between I^- and X^-, etc.) were ignored. The g-values of P^+ and I^-, $g(P^+)$ and $g(I^-)$, are regarded as isotropic and are set equal to one another. We include an isotropic exchange interaction, between I^- and X^-, characterised by the parameter $J(I^-X^-)$. All other exchange interactions, e.g., P^+I^-, P^+X^-, $^3PX^-$, etc., were ignored.

Thus the three-spin Hamiltonian may be written (in angular frequency units):

$$\mathscr{H} = \mu_B B_0 \hbar^{-1}[g S_z^P + g S_z^I + g(X^-) S_z^X] - J(I^-X^-)[\tfrac{1}{2} + 2\mathbf{S}^I \cdot \mathbf{S}^X] \tag{3}$$

where $g = g(P^+) = g(I^-)$, B_0 is the magnetic field strength and μ_B is the Bohr magneton. $\mathbf{S}^A$ and S_z^A represent the spin angular momentum operator and its z component for spin A ($A = P, I, X$), respectively. This Hamiltonian has two very similar 3×3 blocks of non-zero matrix elements corresponding to the states: $S\alpha$, $T_0\alpha$, $T_{-1}\beta$ and $S\beta$, $T_0\beta$, $T_{-1}\alpha$:

$$\begin{array}{c} \\ <S\alpha| \\ <T_0\alpha| \\ <T_{+1}\beta| \end{array} \begin{array}{c} \begin{array}{ccc} |S\alpha> & |T_0\alpha> & |T_{+1}\beta> \end{array} \\ \left[\begin{array}{ccc} \Delta_X - J/2 & J/2 & -J/\sqrt{2} \\ J/2 & \Delta_X - J/2 & -J/\sqrt{2} \\ -J/\sqrt{2} & -J/\sqrt{2} & 2\Delta - \Delta_X \end{array}\right] \end{array} \tag{4}$$

$$\begin{array}{c} \\ <S\beta| \\ <T_0\beta| \\ <T_{-1}\alpha| \end{array} \begin{array}{c} \begin{array}{ccc} |S\beta> & |T_0\beta> & |T_{-1}\alpha> \end{array} \\ \left[\begin{array}{ccc} -\Delta_X - J/2 & -J/2 & J/\sqrt{2} \\ -J/2 & -\Delta_X - J/2 & -J/\sqrt{2} \\ J/\sqrt{2} & -J/\sqrt{2} & -2\Delta + \Delta_X \end{array}\right] \end{array} \tag{5}$$

where

$$\Delta = \tfrac{1}{2} g \mu_B B_0/\hbar$$

$$\Delta_X = \tfrac{1}{2} g(X^-) \mu_B B_0/\hbar$$

$$J = J(I^-X^-) \tag{6}$$

All other matrix elements of $\mathscr{H}$ are equal to zero apart from:

$$<T_{+1}\alpha|\mathscr{H}|T_{+1}\alpha> = 2\Delta + \Delta_X - J$$

$$<T_{-1}\beta|\mathscr{H}|T_{-1}\beta> = -2\Delta - \Delta_X - J \tag{7}$$

Thus the electron on X^- plays essentially the same role as the numerous magnetic nuclei on P^+

and I^-, namely to mix singlet and triplet radical pair states. For this reason and also because $J(I^-X^-)$ (at least in *Rhodopseudomonas viridis* [18]) is much larger than any hyperfine coupling in these radicals, nuclei were excluded from the calculation. It should be noted that at high fields, hyperfine interactions can only cause significant mixing of S and T_0 states of P^+I^- [16,19,20]. whereas, because of the larger Zeeman interaction of the electron, the I^+X^- exchange interaction couples the S state with T_{-1} and T_{-1} as well as T_0 [21]. This is the essential difference between unreduced or quinone-depleted and pre-reduced reaction centres, which leads ultimately to modification of the normal AEEAAE pattern.

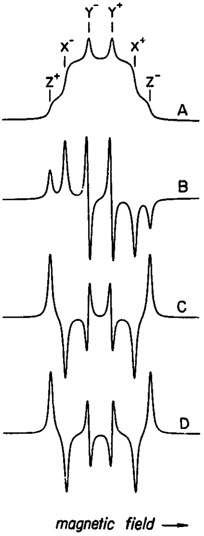

Fig. 1. Schematic EPR spectra of the donor triplet state, ^3P, in *Rps. viridis*. (A) Unpolarized spectrum (χ''). (B) Unpolarized first-derivative ($d\chi''/dB$) spectrum (AAAAAA). (C) Low-temperature, polarized first-derivative spectrum (AEEAAE). (D) High-temperature, polarized first-derivative spectrum (AEAEAE). (D) High-temperature, polarized first-derivative spectrum (AEAEAE).

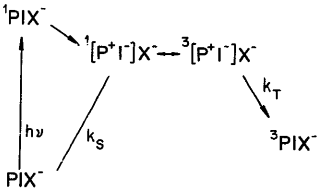

Fig. 2. Simplified reaction scheme for blocked photosynthetic reaction centres.

The next step is to introduce chemical reactivity. The essential events (Fig. 2) are the formation of the radical pair P^+I^- in a singlet state and the collapse of $^3[P^+I^-]$ in state $|m_S>$ to give ^3P in state $|m_S>$. The former is assumed to be instantaneous. The latter is assigned a first-order rate constant k_T (independent of m_S). The reaction of $^1[P^+I^-]$ to give P in its electronic ground state (Fig. 2) is assumed to be negligibly slow ($k_S = 0$) in agreement with the nearly 100% quantum yield of ^3P at low temperatures [22].

Finally, we introduce spin relaxation, without which there can be no inversion of polarization in this simple model. Except at the lowest temperatures, Fe^{2+} will relax rapidly and induce efficient relaxation in Q_A^- to which it is strongly coupled. To model this process, we let X^- undergo spin-lattice relaxation at a rate: $T_1^{-1} = k_R$ and ignore the equilibrium population difference between the $m_S = \pm \frac{1}{2}$ states. Cross relaxation of I^- and X^- is ignored for the moment. Spin–spin relaxation of X^- may also be ignored because the Hamiltonian has no non-zero matrix elements of the type $<q\alpha|\mathscr{H}|q\beta>$ ($q = S, T_{+1}, T_0, T_{-1}$) and so cannot give rise to a coherent superposition of the $m_S = \pm \frac{1}{2}$ states of X^-. Thus X^- has no transverse magnetization to be relaxed.

Putting together the spin evolution, chemical reactivity and relaxation, one obtains the following differential equation for the time dependence

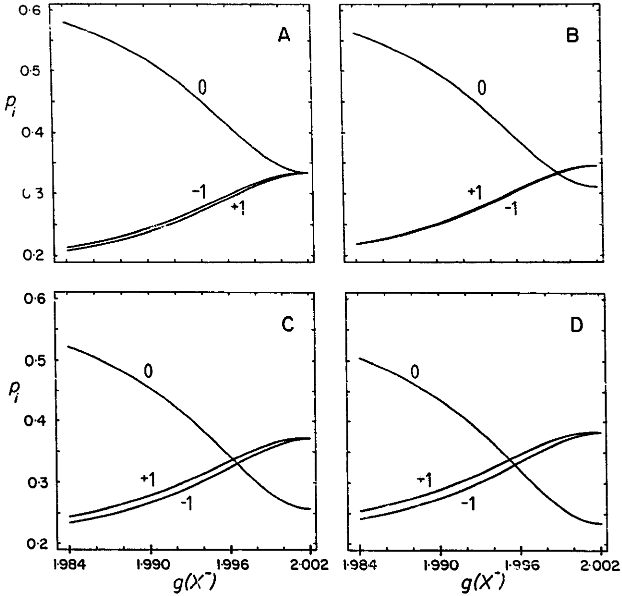

Fig. 3. Calculated relative populating rates of ^{3}P in states T_{+1}, T_0 and T_{-1} as a function of $g(X^-)$. (A) $k_R = 0$; (B) $k_R = 10^8$ s^{-1}; (C) $k_R = 10^9$ s^{-1}; (D) $k_R = 10^{10}$ s^{-1}. Other parameters: $g(P^+) = g(I^-) = 2.002$; $k_T = 3 \cdot 10^9$ s^{-1}; $J(I^- X^-) = -20.0$ mT.

of ρ, the density operator for the three-spin system $P^+I^-X^-$:

$$\frac{d\rho}{dt} = -i[\mathcal{H},\rho] - \tfrac{1}{2}k_T[\mathcal{P}^T\rho + \rho\mathcal{P}^T] + \mathcal{R}\rho \qquad (8)$$

$\mathcal{P}^T$ is the triplet projection operator:

$$\begin{aligned}\mathcal{P}^T = {} & |T_{+1}\alpha\rangle\langle T_{+1}\alpha| + |T_0\alpha\rangle\langle T_0\alpha| + |T_{-1}\alpha\rangle\langle T_{-1}\alpha| \\ & + |T_{+1}\beta\rangle\langle T_{+1}\beta| + |T_0\beta\rangle\langle T_0\beta| \\ & + |T_{-1}\beta\rangle\langle T_{-1}\beta| \qquad (9)\end{aligned}$$

which projects out the triplet components of P^+I^-. $\mathcal{R}$ is a Redfield-type superoperator describing the relaxation of X^-. This equation is solved numerically [21,23] using the initial condition:

$$\rho(0) = \tfrac{1}{2}|S\alpha\rangle\langle S\alpha| + \tfrac{1}{2}|S\beta\rangle\langle S\beta| \qquad (10)$$

to give the relative amounts of ^{3}P in states $|+1\rangle$, $|0\rangle$ and $|-1\rangle$ at a time long compared to the lifetime of P^+I^-, but short compared to the relaxation and decay times of ^{3}P. These quantities are simply the relative populating rates (p_{+1}, p_0 and p_{-1}) of the three states (defined such that $p_{+1} + p_0 + p_{-1} = 1$). The differences $p_0 - p_{+1}$ and $p_{-1} - p_0$ are thus proportional to the initial electron spin polarizations observed in a time-resolved EPR experiment.

Results

Fig. 3 shows the calculated p_i ($i = +1, 0, -1$) of ^{3}P in the three states $|+1>$, $|0>$ and $|-1>$ as a function of $g(X^-)$ for four values of the relaxation rate, k_R. In all the calculations described here the rate of formation of ^{3}P, k_T, was $3 \cdot 10^8$ s^{-1} and $g = g(P^+) = g(I^-)$ was 2.002. For Fig. 3, a value of -20.0 mT for $J(I^-X^-)$ was chosen to match the experimental value for *Rps. viridis* [18]. In this diagram the relative populating rates for $g(X^-) \leqslant g$ are shown: symmetrical behaviour is found for $g(X^-) > g$ (except that the T_{+1} and T_{-1} labels are interchanged).

In Fig. 3A, where $k_R = 0$, the populating rate of the central state $|0>$ is always greater than (or, when $g(X^-) = g$, equal to) the rates for $|+1>$ and $|-1>$. However as k_R increases (Fig. 3B, C and D) p_0 falls below p_{+1} and p_{-1} over a range of g-values close to 2.002. This corresponds to inversion of initial polarization in the EPR spectrum of ^{3}P.

To determine which relaxation pathways are important, the triplet yields were computed under identical conditions but with the spin-lattice relaxation rate between $T_0\alpha$ and $T_0\beta$ and between $S\alpha$ and $S\beta$ reduced to zero. The results differ only slightly from those of Fig. 3. However when, instead, spin-lattice relaxation between $T_{+1}\alpha$ and $T_{+1}\beta$ and between $T_{-1}\alpha$ and $T_{-1}\beta$ is removed, the inversion effect disappears, for all values of k_R, and the graphs of p_i against $g(X^-)$ are essentially identical to Fig. 3A. (i.e. $k_R = 0$).

Finally, the relative populating rates were calculated under the same conditions as Fig. 3 but with a much smaller value of $J(I^-X^-)$. For $J(I^-X^-) = -0.2$ mT, the inversion effect almost disappears (Fig. 4).

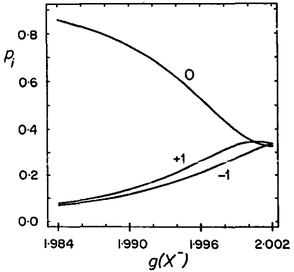

Fig. 4. Calculated relative populating rates of ^{3}P in states T_{+1}, T_0 and T_{-1} as a function of $g(X^-)$ for $J(I^-X^-) = -0.2$ mT. Other parameters: $k_R = 10^{10}$ s^{-1}; $g(P^+) = g(I^-) = 2.002$; $k_T = 3 \cdot 10^8$ s^{-1}.

Discussion

The previous paragraphs describe the results of calculations based on a model photosynthetic reaction centre. The aim was to elucidate the anisotropic inversion of electron spin polarization observed for ^{3}P in pre-reduced *Rps. viridis* reaction centres at temperatures above about 20 K. In this simple approach, inversion of initial polarization is predicted whenever the populating rate of ^{3}P in its $m_S = 0$ state (p_0) is smaller than both p_{+1} and p_{-1}, the populating rates for the $m_S = \pm 1$ states. It has been shown that p_{+1} and p_{-1} are indeed larger than p_0 when the three conditions are fulfilled: the g-value of X^- is close to those of P^+ and I^-; the exchange interaction of I^- with X^- is large; and X^- undergoes rapid spin-lattice relaxation.

Before commenting on the connection between these results and the experimental observations, we first attempt to rationalise them in a simple qualitative way. The argument is couched in terms of the $S\alpha$, $T_0\alpha$, $T_{+1}\beta$, etc., basic states of the $P^+I^-X^-$ three-spin system. To simplify matters we ignore off-diagonal elements of the three-spin density matrix and concentrate on the diagonal elements, which give the probabilities of finding the spin system in each of the basic states. As we shall demonstrate, a satisfactory physical picture of what is happening can be developed without reference to coherent superpositions of the basic states.

Let us first discuss what happens in the absence of relaxation. From the structure of the Hamiltonian (Eqns. 4–7) one can see that states $T_{+1}\beta$, $T_0\alpha$, $T_0\beta$ and $T_{-1}\alpha$ become populated by virtue of the I^-X^- exchange interaction, but that $T_{+1}\alpha$ and $T_{-1}\beta$, which are not connected by $\mathscr{H}$ to any of the other states, do not. When $|\Delta - \Delta_X| \gg |J|$, $T_{+1}\beta$ is not strongly mixed with $S\alpha$ because the mixing term $|<S\alpha|\mathscr{H}|T_{+1}\beta>|$ is then much smaller than the difference in diagonal matrix elements $<S\alpha|\mathscr{H}|S\alpha> - <T_{+1}\beta|\mathscr{H}|T_{+1}\beta>|$. Similarly, there is little indirect mixing via $T_0\alpha$ because $<T_0\alpha|\mathscr{H}|T_{+1}\beta\beta>|$ is small compared to $|<T_0\alpha|\mathscr{H}|T_0\alpha> - <T_{+1}\beta|\mathscr{H}|T_{+1}\beta>|$. Similar arguments apply to mixing of $T_{-1}\alpha$ with $S\beta$ and $T_0\beta$. So, when $|\Delta - \Delta_X| \gg |J|$ the radical pair P^+I^- never acquires much T_{+1} or T_{-1} character, and hence p_{+1} and p_{-1} are much less than p_0. When $\Delta = \Delta_X$, it turns out that the mixing of $S\alpha$ ($S\beta$) with $T_{+1}\beta$ ($T_{-1}\alpha$) is exactly twice as strong as it is with $T_0\alpha$ ($T_0\beta$). Remembering that $T_{+1}\alpha$ and $T_{-1}\beta$ are not populated at all when $k_R = 0$, this means that $p_{+1} = p_0 = p_{-1}$. Fig. 3A shows clearly the equality of the three populating rates when $g = g(X^-)$ and the drop in p_{+1} and p_{-1} when $g(X^-)$ differs from g.

When X^- undergoes spin-lattice relaxation, however, the situation is changed. The formation of $T_{+1}\alpha$ and $T_{-1}\beta$ from $T_{+1}\beta$ and $T_{-1}\alpha$, respectively, opens up the possibility of a new pathway to the $|+1>$ and $|-1>$ states of ^3P. Clearly this will only be significant when there are reasonable amounts of $T_{+1}\beta$ and $T_{-1}\alpha$ in the first place, which in turn requires that $|\Delta - \Delta_X|$ is not large compared to $|J|$ as discussed above. Under these circumstances, radical pairs that would have proceeded via $T_0\alpha$ and $T_0\beta$ to give ^3P in its $|0>$ state are diverted along the new routes via $T_{+1}\alpha$ and $T_{-1}\beta$. In this way, the number of radical pairs reacting separately via the T_{+1} and T_{-1} routes may exceed the number going through T_0.

One can see that k_R must be greater than or similar to k_T to get much inversion. When this is not the case, all of the radical pairs will have disappeared before there is time to populate $T_{+1}\alpha$ and $T_{-1}\beta$ by relaxation. Fig. 5 summarizes the important reaction pathways in the absence and presence of spin-lattice relaxation.

The above interpretation is supported by the time dependence of the yields of $^3PX^-$ in each of its six states (labelled $|+1\alpha>$, $|+1\beta>$, $|0\alpha>$, $|0\beta>$, $|-1\alpha>$, $|-1\beta>$ to distinguish them from the states of $P^+I^-X^-$). Fig. 6A and B shows these yields as a function of time for $g(X^-) = 2.002$ and 1.990, respectively, in the absence of relaxation, with $k_T = 3 \cdot 10^8$ s^{-1} and $g = 2.002$. Note that the asymptotic values of these yields give the relative populating rates of the various states. The behaviour described above can clearly be seen from these graphs: the states $|+1\alpha>$ and $|-1\beta>$ are not produced; when $\Delta = \Delta_X$ (Fig. 6A) $|+1\beta>$ and $|-1\alpha>$ are formed exactly twice as fast as $|0\alpha>$ and $|0\beta>$; when $|\Delta - \Delta_X| > 0$ (Fig. 6B) the formation of $|0\alpha\beta$ and $|0\beta>$ is favoured at the expense of $|+1\beta>$ and $|-1\alpha>$. In addition, it is clear from these curves that spin-lattice relaxation between the radical pair states $T_0\alpha$ and $T_0\beta$ is indeed unlikely to be important because their populations (as reflected by the yields of $|0\alpha>$ and $|0\beta>$) are very similar. The oscillations on the rising parts of the curves result from the coherent interconversion of singlet and triplet radical pair states.

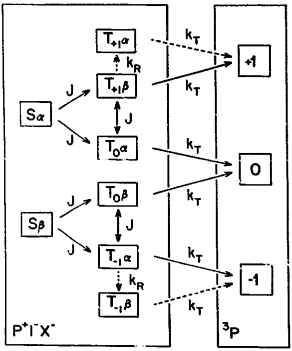

Fig. 5. The important pathways involved in the reactions: $^1[P^+I^-]X^- \rightarrow {^3[P^+I^-]X^-} \rightarrow {^3PIX^-}$. The steps indicated by dashed arrows are only important when X^- undergoes rapid spin-lattice relaxation. The three types of interconversion are labelled as follows: J, coherent mixing mediated principally by $J(I^-X^-)$: k_R, spin lattice relaxation of X^-; k_T, electron-hole recombination of P^+I^-.

The time dependence in the presence of relaxation ($k_R = 10^9$ s^{-1}) is shown in Fig. 6C and D for $g(X^-) = 2.002$ and 1.990, respectively. In both cases the yields of $|+1\alpha>$ and $|-1\beta>$ are appreciable and there is a corresponding drop in the amounts of the other four states. When $\Delta = \Delta_X$ (Fig. 6C) the yields of $|0\alpha>$ and $|0\beta>$ are most strongly affected while the opposite is true for larger $|\Delta - \Delta_X|$ (Fig. 6D). The former corresponds to inversion, the latter does not. The slightly sigmoidal growth of the populations of $|+1\alpha>$ and $|-1\beta>$ in Figs. 6C and 6D reflect the indirect formation of the corresponding radical pair states, by relaxation.

Conclusion

In the preceding pages we have indicated how rapid spin-lattice relaxation of X^- can alter and, under the right conditions, invert the electron spin polarization of ^3P. We now make the connection

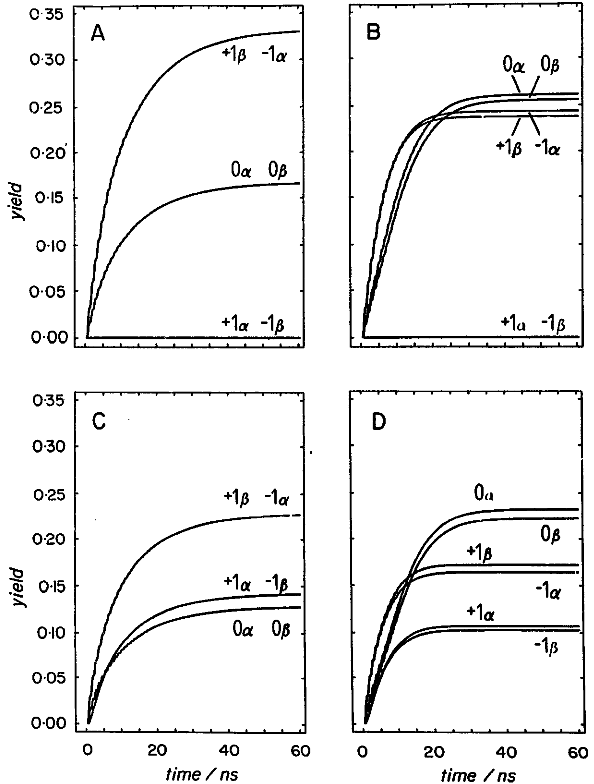

Fig. 6. Calculated yields of $^3PX^-$ in each of the states $|+1\alpha>$, $|+1\beta>$, $|0\alpha>$, $|0\beta>$, $|-1\alpha>$, $|-1\beta>$ as a function of time. (A) $g(X^-)=2.002$, $k_R=0$; (B) $g(X^-)=1.990$ $k_R=0$; (C) $g(X^-)=2.002$, $k_R=10^9$ s^{-1}; (D) $g(X^-)=1.990$, $k_R=10^9$ s^{-1}. Other parameters: $J(I^-X^-)=-20.0$ mT; $g(P^+)=g(I^-)=2.002$; $k_T=3\cdot10^8$ s^{-1}.

to the experimental observation (part I: Ref. 28) that the initial polarization changes from AEEAAE at 8 K to –EAEA– at 100 K. The above treatment is based on a drastically simplified model of the bacterial reaction centre. We should not expect, therefore, to be able to account quantitatively for this observation. However, qualitatively, we can see that two conditions must be satisfied. First, the rate of spin-lattice relaxation in X^- must become comparable to k_T at a temperature close to 20 K. Second, to account for the inversion of the Y peaks and the loss of signal for the Z peaks, the effective *g*-value of X^- should be reasonably close to 2.002 when the magnetic field is directed along the Y axis of ^3P; very different from 2.002 when the field is along the X axis and of an intermediate value for the Z axis. We comment on these separately.

Not much appears to be known about the spin relaxation of Fe^{2+} in photosynthetic reaction centres. However, there is some evidence for a substantial increase in the relaxation rate around 15 K [8,24]. The light-induced EPR spectrum of $Q_A^-Fe^{2+}$ at liquid helium temperatures is a broad signal (width 640 ± 30 G) centred at $g = 1.8$. At 20 K the line is appreciably broadened and by 30 K it is difficult to observe [25]. The most obvious source of these effects is rapid spin relaxation.

The anisotropy of the EPR spectrum of X^- is less straightforward. As yet, there have been no reports of the angular dependence of the EPR frequency in single crystals. However, from the spectra of randomly oriented *Rhodobacter sphaeroides* reaction centres, Butler et al. [25] argue persuasively that the resonance frequency of $Q_A^-Fe^{2+}$ is indeed strongly anisotropic and inhomogeneously broadened with resonances covering the range $g \approx 0.8$ to $g \approx 5.0$. Strong support for this conclusion is provided by the work of Dismukes et al. on oriented cells of *Rps. viridis* [26]. So, for some orientations of the reaction centre the EPR absorption must occur near $g = 2$. If these orientations are also those for which the magnetic field is directed along the Y axis of ^3P, then inversion of the Y peaks would be expected.

Further work is clearly needed to clarify the processes underlying the anisotropic inversion of polarization in ^3P. For example cross relaxation of I^- and X^- has not been discussed. Preliminary work indicates that relaxation of I^- caused by rapid spin-lattice relaxation of X^- (scalar relaxation of the second kind [27]) widens the range of *g*-values over which inversion is predicted but decreases the size of the effect by tending to equalise the populating rates of the three levels of ^3P. Other aspects that need to be considered include anisotropic relaxation of X^- and the anisotropic interaction of I^- and X^-.

Acknowledgement

D.A.H. is grateful to the Science and Engineering Research Council for a research studentship.

References

1 Dutton, P.L., Leigh, J.S. and Siebert, M. (1972) Biochem. Biophys. Res. Commun. 46, 406–413.

2 Thurnauer, M.C., Katz, J.J. and Norris, J.R. (1975) Proc. Natl. Acad. Sci. (USA) 72, 3270–3274.

3 Hoff, A.J. (1979) Phys. Reports 54, 75–200.

4 Hoff, A.J. (1982) Biophys. Struct. Mech. 8, 107–150.

5 Hoff, A.J. (1984) Q. Rev. Biophys. 17, 153–282.

6 Van Wijk, F.G.H., Gast, P. and Schaafsma, T.J. (1986) Photobiochem. Photobiophys. 11, 95–100.

7 Van Wijk, F.G.H., Gast, P. and Schaafsma, T.J. (1986) FEBS Lett. 206, 238–242.

8 Van Wijk, F.G.H., Beijer, C.B., Gast, P. and Schaafsma, T.J. (1987) Photochem. Photobiol. 46, 1015–1019.

9 Van Wijk, F.G.H. (1987) Thesis, Wageningen Agricultural University.

10 Holten, D., Windsor, M.W., Parson, W.W. and Thornber, J.P. (1978) Biochim. Biophys. Acta 501, 112–127.

11 Windsor, M.W. and Holten, D. (1980) Phil. Trans. R. Soc. Lond. A 298, 335–349.

12 Wertz, J.E. and Bolton, J.R. (1986) Electron Spin Resonance, pp. 238–242, Chapman and Hall, London.

13 Muus, L.T., Atkins, P.W., McLauchlan, K.A. and Pedersen, J.B. (eds.) (1977) Chemically Induced Magnetic Polarization, Reidel, Dordrecht.

14 Salikhov, K.M., Molin, Yu.N., Sagdeev, R.Z. and Buchachenko, A.L. (1984) Spin polarization and magnetic effects in radical reactions (Molin, Yu.N., ed.), Elsevier, New York.

15 Boxer, S.G., Chidsey, C.E.D. and Roelofs, M.G. (1983) Annu. Rev. Phys. Chem. 34, 389–417.

16 Hoff, A.J. (1981) Q. Rev. Biophys. 14, 599–665.

17 Butler, W.F., Johnston, D.C., Shore, H.B., Fredkin, D.R., Okamura, M.Y. and Feher, G. (1980) Biophys. J. 32; 967–992.

18 Prince, R.C., Tiede, D.M., Thornber, J.P. and Dutton, P.L. (1977) Biochim. Biophys. Acta 462, 467–490.

19 Werner, H.-J., Schulten, K. ad Weller, A. (1978) Biochim. Biophys. Acta 502, 255–268.

20 Haberkorn, R. and Michel-Beyerle, M.E. (1979) Biophys. J. 26, 489–498.

21 Hoff, A.J. and Hore, P.J. (1984) Chem. Phys. Lett. 108, 104–110.

22 Wraight, C.A., Leigh, J.S., Dutton, P.L. and Clayton, R.K. (1974) Biochim. Biophys. Acta 333, 401–408.

23 De Kanter, F.J.J., Den Hollander, J.A., Huizer, A.H. and Kaptein, R. (1977) Mol. Phys. 34, 857–874.

24 Calvo, R., Butler, W.F., Isaacson, R.A., Okamura, M.Y., Fredkin, D.R. and Feher, G. Biophys. J. 37, 111a.

25 Butler, W.F., Calvo, R., Fredkin, D.R., Isaacson, R.A., Okamura, M.Y. and Feher, G. (1984) Biophys. J. 45, 947–973.

26 Dismukes, G.C., Frank, H.A., Friesner, R. and Sauer, K. (1984) Biochim. Biophys. Acta 764, 253–271.

27 Abragam, A. (1961) The Principles of Nuclear Magnetism, Oxford University Press, Oxford.

28 Van Wijk, F.G.H. and Schaafsma, T.J. (1988) Biochim. Biophys. Acta 936, 236–248.